Unique Features of the University of Maryland Electron Ring and the Necessity of PIC Code Simulation

R. A. Kishek, S. Bernal, M. Venturini, and M. Reiser,
Institute for Plasma Research, University of Maryland, College Park, MD 20742
I. Haber, Naval Research Laboratory, Washington, DC 20375
D. P. Grote, Lawrence Livermore National Lab, Livermore, CA

Abstract.

The Maryland Electron Ring [1] is designed to explore the transport of beams with much higher space charge than other circular machines. In addition, the ring functions as a testbed for design and simulation codes. Applications such as Heavy Ion Fusion and High Intensity Colliders require the preservation of beam quality during transport over large distances. This paper describes the application of self-consistent particle-in-cell code simulations using the WARP suite [2] to the E-ring lattice. The model used includes the nonlinear details of the external magnetic fields, a cylindrical external conductor, and the dispersive effects of the circular lattice on a beam with a non-zero energy spread.

1. INTRODUCTION

In the accelerator field, many applications are emerging that require high intensities and good beam quality. Heavy Ion Fusion, for example, requires the transport and acceleration of a high current beam and focusing it onto a tiny spot. Spallation neutron sources and high intensity colliders also require good beam quality, although the intensities needed may be somewhat lower. Furthermore, most of these applications involve some degree of bending of the beam, and some can benefit from the concept of a recirculator to save space and costs. The University of Maryland Electron Ring [1], which is currently in its early construction stages, is a scaled experiment designed to investigate the physics of space-charge dominated beams in a circular geometry. A key goal of the project is its low cost, driving us to use innovative features such as printed-circuit magnets [3] and modularity in design.

Since the E-ring is to be operated in regions of high space-charge previously inaccessible to circular machines, a high priority in this project rests on self-consistent computer simulations to verify the design and further probe the physics. In the on-going process leading up to the commissioning of the ring, the numerical simulations are benchmarked against any experimental measurements available. Because of its low cost and versatility, the E-ring will provide a valuable testbed for computer codes to be used in designing larger machines.

In ref. [4] we had presented results of preliminary simulations in a straight alternating-gradient channel including the magnet nonlinearities. In ref. [5] we extended the simulations to follow the beam along the bent lattice, examining the consequences of lens non-linearities, mismatches, and dispersion on the beam quality. In this paper, we will expand on some of the features of the E-ring that necessitate the use of particle-in-cell (PIC) methods, then proceed to describe some interesting results observed in the simulations.

In the simulations described herein, we rely primarily on the WARP particle-in-cell (PIC) code [2], which has been developed at Lawrence Livermore National Laboratory for Heavy Ion Fusion applications. An important feature of the WARP code is its ability to efficiently track a space-charge-dominated beam along bends. The particle orbits are integrated self-consistently using the fully nonlinear electrostatic self-field, as well as the fully nonlinear external fields from the bending dipoles and focusing quadrupoles. The WARP code is an attractive choice for the Maryland ring simulations especially because it has been used in simulating the similar Heavy Ion Recirculator at Lawrence Livermore National Lab [2], and is therefore well-suited to such geometries and already contains a variety of lattice element representations.

2. RING LATTICE AND SIMULATION SETUP

The design and progress of the electron ring project have been described more fully elsewhere [1]. For the purposes of this paper, it will be sufficient to briefly describe the lattice and nominal beam parameters. The nominal beam current is 100 mA at 10 keV, resulting in a generalized perveance of 0.0015. A nominal (unnormalized 4*rms) emittance of 50 mm-mrad and nominal average beam radius of 10.2 mm (σ_o = 72°) results in a tune depression (ν / ν_o) of 0.16, placing the beam in the strongly space-charge-dominated regime. A future phase is planned where the beam is to be accelerated to 50 keV. Moreover, the ring is designed to run at lower beam currents, allowing us to explore a wide range of tunes.

Figure 1 displays a schematic of the ring lattice, which consists of 36 FODO cells around the 11.52 m circumference ring. Each cell is therefore 32.0 cm long

and contains two evenly-spaced printed-circuit quadrupoles [3] and, in between those, a printed-circuit dipole which bends the beam by 10°. The quadrupole gradient is about 0.078 Tesla/m, while the bending dipole peak field is about 0.00154 Tesla. Three induction gaps used for longitudinal confinement are evenly distributed around ring, while the remainder of the spaces are occupied by diagnostics and pumping ports.

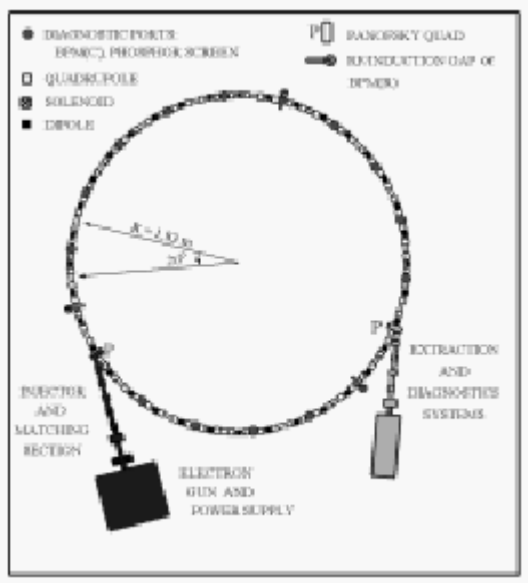

Figure 1. Schematic of ring design [1].

Because of space limitations in the mechanical design, the quadrupoles and the dipoles are short relative to the pipe radius (effective length of both ~ 3.7 cm; pipe radius ~ 2.5 cm). Indeed, as Figure 2 shows, the quadrupoles and dipoles consist almost entirely of fringe fields. Although the external fields were designed to be linear in an integrated sense, the question arises whether they may be nonlinear when integrated over the actual particle orbits, and whether such nonlinearities lead to emittance growth. PIC methods that self-consistently include the space charge are powerful tools in answering such questions.

The short effective length of the dipoles implies that the lattice can be thought of as a combination of bends and straight sections. In other words the local radius of curvature of the reference orbit varies as a function of the propagation distance, s, inside the bend. Furthermore, for induction accelerators, the dominant cost-driving factor is the size of the induction cores, which is partly determined by the bore size and hence the beam size. This expense can be reduced if the beam fills a large cross-section of the beam pipe, but at the expense of image forces. In the Maryland E-ring the ratio of beam radius to pipe radius is about 2/5, and so, as explained below, the image forces are non-negligible and must be implemented carefully into the model.

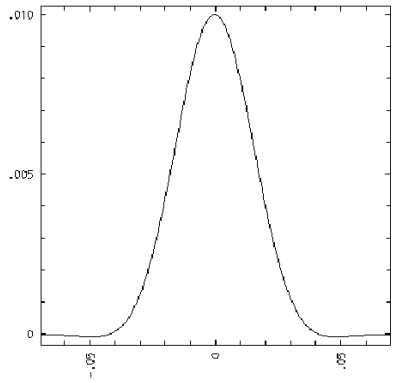

Figure 2. Profile of printed-circuit quadrupole on-axis gradient as a function of z.

Since a beam, in general, has a non-zero energy spread, propagation in bends leads to dispersion, i.e., particles at different energies oscillate around different reference trajectories. If not explicitly matched for dispersion, the beam experiences a dispersion mismatch as it enters the ring from the straight injector, or as it leaves it to the extraction section. For a space charge dominated beam, this dispersion mismatch leads to emittance growth, as confirmed earlier by theory and simulation [6-7, 5]. Further studies described below demonstrate that dispersion is more pronounced for space-charge-dominated beams and show the dependence.

For these simulations of the transverse dynamics, we use WARP-XY, the single-slice version of WARP, which solves for the self-fields on a 2-D mesh, but retains the velocity information in all 3 dimensions [2]. The lattice is modeled from first principles by computing the lens magnetic field values on a 3D grid with the aid of a magnetics program, starting with the actual conductor geometry. At every step, WARP interpolates this field data to the particle locations. Thus the dipoles and quadrupoles used in the simulation include the nonlinearities caused by the fringe fields. We load a beam with an initial semi-Gaussian distribution into the field-free region between two quadrupoles, and then follow its evolution along s, the distance traversed by the beam, for a number of turns (typically 10). The beam is initially rms matched into the lattice using the standard rms envelope equations [8].

The numerics have been thoroughly tested to ensure convergence. A mesh of 256×128 cells across the 5 cm-diameter pipe (symmetry in the vertical direction halves the number of cells needed) provides sufficient resolution of Debye-length-scale variations in the potential. The number of simulation particles is chosen to minimize effects of numerical collisions, producing a

potential that is relatively smooth from cell to cell. Up to 400k particles have been used in some simulations, although it is found that for most purposes, 100k particles are sufficient. Gaussian filtering (see [9]) allows us to get convergent results with even fewer particles (~ 10k). The time step used corresponds to a beam advance by 0.4 cm, which is enough to resolve the fringe fields of the magnets. In addition, we continually benchmark WARP against emerging experimental measurements from prototypes of the ring and the injector. Agreement, which has been excellent so far, is discussed elsewhere [10].

3. SIMULATION RESULTS AND DISCUSSION

3.1 Magnet nonlinearities

In ref. [4] we had presented the scaling of emittance growth in a straight channel with the number of particles, indicating that whatever growth present is numerical in nature and can be eliminated by increasing the number of particles. In fact, the nonlinearities from the fringe fields of the short quadrupoles are found to contribute very little to the emittance growth. This can also be demonstrated by replacing the full description of the magnets in the model with ideal, hard-edge elements. As Fig. 3 indicates, there is little difference between the two cases, so the assumption that the quadrupole fields are linear when integrated over particle orbits is correct. This is true because, by design, the quadrupole fields are linear when integrated along z, and the quadrupoles are short enough compared to the (depressed) betatron period that the radii of particle orbits do not change significantly.

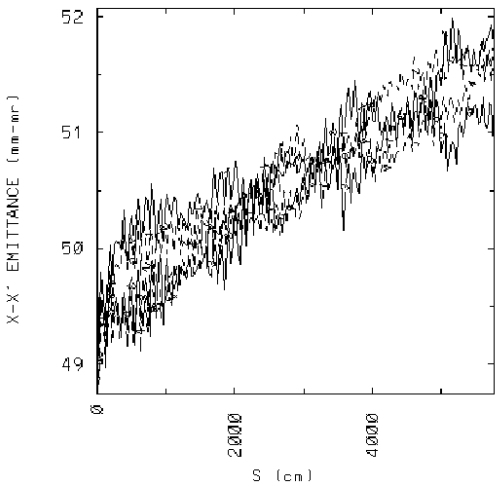

Figure 3. Evolution of a matched beam with the nominal design parameters in a straight A-G channel over 360 lattice periods, for nonlinear (solid) vs. ideal quadrupoles (dotted). Value of 4*rms x and y emittances strobed every lattice period in between quadrupoles.

The dipoles, however, are a different matter. After the addition of bends and dipole fields into the WARP model, we observe a somewhat larger emittance growth [dotted lines in Fig. 4]. Although the emittance growth rate is not excessive (30 % over 10 turns after subtracting numerical growth), it is important to understand its causes. [The small short-term emittance growth at the beginning is due to a dispersion mismatch; it can be removed by launching a beam with a smaller energy spread].

Numerical tests suggest that this growth in emittance is real. Although the study conducted so far is by no means exhaustive, we have reasons to believe that this emittance growth is related to the interaction of the beam space charge with the dipole nonlinearities. For instance, in some simulations, we applied appropriate scaling to reduce the effects of the dipole nonlinearities experienced by the beam. This was accomplished by reducing both the beam current and emittance in order to reduce the beam size while maintaining both the matched condition and the tune depression. The boundaries were also shifted to maintain the contribution of the image forces, while the numerics were adjusted to maintain the same resolution and collisionality.

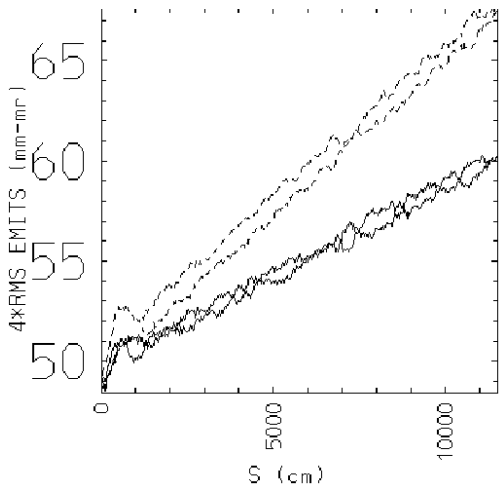

Figure 4. Evolution of a matched beam in the ring over 10 turns (360 lattice periods). The dotted line represents a beam with the nominal design parameters while the solid line represents a beam scaled by a factor of 1/2 to reduce the effects of dipole nonlinearities. Value of 4*rms x and y emittances strobed every lattice period in between quadrupoles. Here, ideal quadrupoles are used to isolate the effects of the dipoles.

The result of this test is that the smaller beam, which samples less of the dipoles' deviations from linearity, exhibits a significantly smaller emittance growth [solid lines in Fig. 4]. The question arises as to why the dipoles, which were also designed to be linear in

the integrated sense, lead to more emittance growth than the quadrupoles. There are two differences worth noting, however, between the dipoles and the quadrupoles. First, the dipoles are typically operated with somewhat stronger fields than the quads (the dipole field is a factor of 2 more than the quad field at the edge of the beam). The second is that the beam, hence the individual particles, follows a curved trajectory inside the dipole, whereas the dipole fields were designed to be linear when integrated along z, the dipole axis. This difference is small for a 10° bend, yet nevertheless may add up over a large number of lattice periods. Also note that the space charge plays an important role. An emittance-dominated beam with the same size experiences much less emittance growth.

3.2 Boundaries

As mentioned earlier, the beam fills a relatively large cross-section of the beam pipe. Furthermore, the local radius of curvature of the beam trajectory varies inside each bend, and so even a well-aligned beam departs momentarily from the pipe axis. This makes image effects quite significant. In WARP, a capacity matrix used in conjunction with the FFT field solver is used to represent the cylindrical boundary [2]. The capacity matrix solver was not originally implemented for use inside bends. Hence, when used inside a bend, that model corresponded to leaving a straight beam pipe around the beam. Later modifications to the field solver* refined the capacity matrix implementation to model the beam pipe in the bends as a curved conductor.

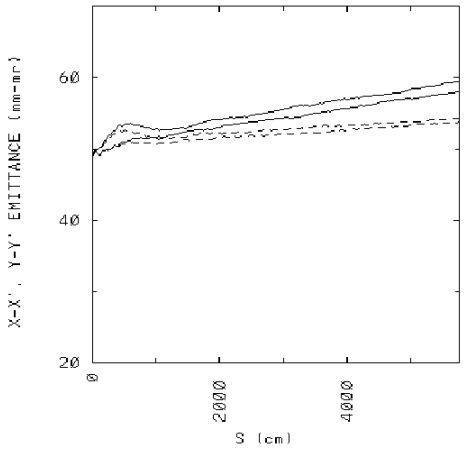

Figure 5. The effect of different implementations of the boundary conditions inside the bend on beam emittance; curved conductors (solid) vs. straight conductors (dotted).

Although the correction is small, the differences add up after propagation through a large number of bends, thus affecting the long-term emittance growth computed by the code. This result is shown in Fig. 5, where we compare the emittance growths from the simulations using the two different implementations of the capacity matrix. Clearly, the different boundaries significantly affect the long-term emittance, resulting in a factor of 2 difference in its growth rate. Therefore, at least for situations like this where the beam covers a large fraction of the pipe cross-section, the boundaries must be accurately represented in order to get accurate answers. This further implies that calculations that totally neglect the boundary may not be as accurate.

3.3 Dispersion

Venturini and Reiser in ref. [6] have derived new envelope equations that are valid in the presence of space charge and dispersions. These equations can be used, for example, to match the beam from a straight injector into a ring. In refs. [5] and [7], WARP simulations have been applied to injection into the Maryland Electron Ring. No attempt has been made to match the dispersion function of the beam, relying instead on the standard RMS envelope equations [8] for matching into the ring. Beams with a spread in energies experience a mismatch in dispersion and an increase in the x-emittance, followed by damped oscillations [Fig. 6]. Incidentally, this result with WARP-3D is almost identical to that obtained from WARP-XY (which uses a different set of approximations), confirming our confidence in the simulation. The simulations were found to be in excellent agreement with the theory presented in ref. [6], except for the eventual exchange of energy between the x and y directions resulting in the damping of the oscillations.

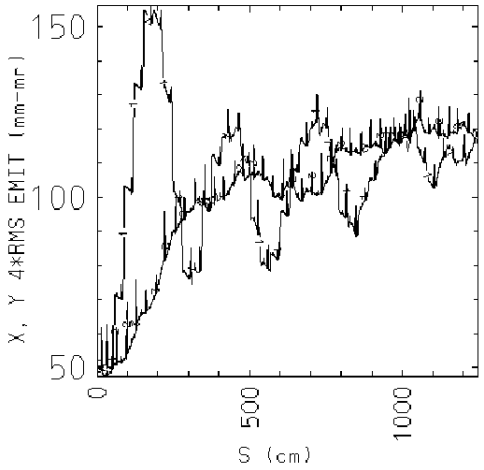

Figure 6. X and y emittances over 1 turn from a 3-D simulation of a beam injected into the ring from a straight lattice with an initial velocity spread ($\Delta v_z/v_z$ = 0.015).

* Done by D. P. Grote at LLNL.

The emittance increase and oscillations are due to a dispersion mismatch.

That study is extended here to test the theory (ref. [6]) for a wider range of parameters. Figure 7 compares the peak of the dispersion function oscillations calculated from the theory to that observed in simulations as function of the beam current. The good agreement confirms the theory for lower tune depressions. Indeed, for lower tune depressions, the damping seen in the simulations occurs over a longer timescale, which increases the region of overlap between the theory and the simulation. Note that the peak of the dispersion function increases almost linearly with the beam current. Since the dispersion function is a measure of the distortion of reference trajectories of particles according to their energy, this result demonstrates that beams with a higher space charge are more susceptible to dispersive effects. In other words, dispersion becomes more important for space-charge-dominated beams.

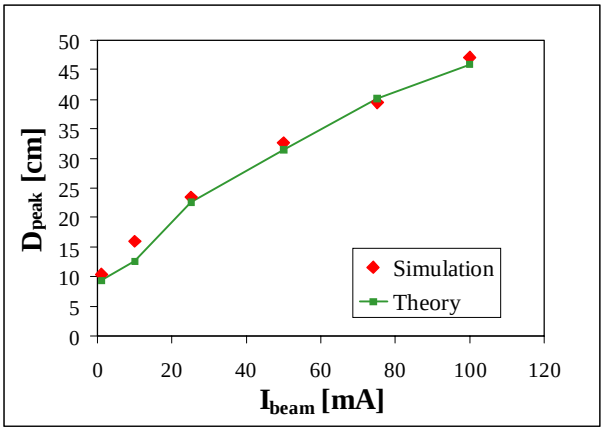

Figure 7. Dependence of peak of dispersion function on beam current for a velocity spread, $\Delta v_z/v_z = 0.015$: theory (solid line) vs. simulation (points).

It is worth noting that Barnard, et. al., at LLNL have proposed a similar theory on dispersion based on the moment description [11]. Although that theory cannot be used to calculate the dynamic evolution of the beam envelope and emittance, their thermodynamic approach provides an accurate estimate of the final beam emittance (i.e., after the oscillations subside) that agrees well with our simulations on the Maryland ring. Barnard's theory also predicts a larger emittance growth from a dispersion mismatch for higher space charge.

4. CONCLUSION

In summary, the Maryland Electron ring contains some unique features that need to be included in a simulation model for a faithful representation of the machine. In this paper we have addressed the magnet nonlinearities, the outer conductor, and the energy spread of the beam. It is found that the effect of the nonlinearities caused by the fringe fields of the short quadrupoles vanish upon integrating along the particle orbits. Those of the short bending dipoles, however, do not completely vanish and lead to an emittance growth after several turns around the ring. We are conducting additional studies to understand the exact mechanism by which the emittance grows in the dipoles. Since the local radius of curvature of the beam trajectory inside the bends is not constant, and since the beam fills a large cross-section of the beam pipe, the image forces cannot be neglected from the model. Finally, a non-zero energy spread leads to dispersion and perhaps to a change in the matching conditions of the beam. Dispersion is seen to affect the beam substantially more at higher currents, in agreement with the applicable theories.

As experimental data becomes available in the forthcoming commissioning process of the E-ring, it will be interesting to compare with the WARP predictions.

ACKNOWLEDGEMENTS

We wish to thank our colleagues John J. Barnard, Alex Friedman, Terry F. Godlove, Steve Lund, and J.G. Wang for many fruitful discussions. The code runs on computers provided by the National Energy Research Scientific Computing Center (NERSC). This research is sponsored by the U. S. Department of Energy (DOE) under contract DE-FG02-94ER40855.

REFERENCES

[1] M. Reiser, S. Bernal, A. Dragt, *et. al.*, Fus. Eng. and Des. **32-33**, 293 (1996); J. G. Wang, S. Bernal, P. Chin, *et. al.*, Nucl. Instr. and Meth. A, **415**, 422-427 (1998).
[2] D. P. Grote, *et. al.*, Fus. Eng. & Des. **32-33**, 193-200 (1996).
[3] T. Godlove, S. Bernal, and M. Reiser, Proc. of 1995 Particle Accelerator Conference, 2117 (1995).
[4] R. A. Kishek, S. Bernal, M. Reiser, *et. al.*, Nucl. Instr. and Meth. A, **415**, 417-421 (1998).
[5] R. A. Kishek, I. Haber, M. Venturini, and M. Reiser, presented at the Workshop on Space-Charge Physics in High Intensity Hadron Rings, Shelter Island, NY, May 4-7, 1998, in print (1999).
[6] M. Venturini and M. Reiser, Phys. Rev. Lett., **81**, 96 (1998);
[7] M. Venturini, R. A. Kishek, and M. Reiser, Proc. Workshop on Space-Charge Physics in High Intensity Hadron Rings, Shelter Island, NY, May 4-7, 1998, in print (1999).
[8] M. Reiser, Theory and Design of Charged Particle Beams, (New York: Wiley & Sons, 1994).
[9] C. K. Birdsall and A. B. Langdon, Plasma Physics through Computer Simulation, (New York: McGraw Hill, 1985).
[10] S. Bernal, P. Chin, R. Kishek, et. al., Phys. Rev. ST Accel. Beams **4**, 044202 (1998); S. Bernal, R. A. Kishek, M. Reiser, and I. Haber, "Observation and Simulation of Radial Density Oscillations in Space-Charge Dominated Electron Beams," to be published (1999).
[11] J. J. Barnard, G. D. Craig, A. Friedman, *et. al.*, Proc. Workshop on Space-Charge Physics in High Intensity Hadron Rings, Shelter Island, NY, May 4-7, 1998, in print (1999).